Pergamon

Tetrahedron: Asymmetry Vol. 6, No. 6, pp. 1375-1386, 1995
Elsevier Science Ltd
Printed in Great Britain
0957-4166/95 $9.50+0.00

0957-4166(95)00170-0

A Predictive Active Site Model for the Cyclohexanone Monooxygenase Catalyzed Oxidation of Sulfides to Chiral Sulfoxides.

Gianluca OTTOLINA[1]*, Piero PASTA[1], Giacomo CARREA[1],

Stefano COLONNA[2], Sabrina DALLAVALLE[2] and Herbert L. HOLLAND[3]

[1]Istituto di Chimica degli Ormoni, C.N.R. Via Mario Bianco 9, 20131 Milano, [2]Istituto di Chimica Organica, Facoltà di Farmacia, Via Venezian 21, Milano, Italy, [3]Department of Chemistry, Brock University, St.Catharines, Ontario, Canada.

Abstract.

An active site model to explain and predict the stereoselectivity of the sultoxidation of organic sulfides to optically active sulfoxides catalyzed by cyclohexanone monooxygenase from *Acinetobacter* NCIB 9871 is proposed. The model is based on cubic-space descriptors and derives from the results obtained with over 30 different sulfides. The model, which also appears to be suitable for explaining the stereoselectivity of cyclohexanone monooxygenase-catalyzed Baeyer-Villiger reactions, is consistent with and expands on the features of other previously described models for the latter process.

Introduction.

Enzymatic oxidation of sulfides[1] is an alternative to chemical asymmetric synthesis[2] for production of optically active sulfoxides, which are compounds of great interest as chirons[3] and stereodirecting groups.[4] In many cases, the enzymes have been used as "black boxes", without any understanding or explanation of the parameters able to influence enantioselectivity or even induce opposite stereoselectivity. This, of course, hinders the application of these enzymes to syntheses.

We have shown previously that cyclohexanone monooxygenase (CMO) from *Acinetobacter* NCIB 9871 can catalyze the asymmetric sulfoxidation of numerous aryl alkyl sulfides (**Scheme**), dialkyl sulfides and dialkyl disulfides.[5a] The structure of the sulfide dramatically influenced not only the enantioselectivity, but also the stereochemical course of the reaction, giving sulfoxides ranging from 99% e.e. with (*R*)-configuration to 93% e.e. with (*S*)-configuration.[5a] Similar results were obtained in the asymmetric oxidation of phenyl alkyl sulfides with the alkyl chain functionalized with Cl, CN vinyl or hydroxyl groups[5b] and of benzyl alkyl sulfides.[5c] As a rule of thumb, introduction of substituents in the aromatic ring or increasing the size of the alkyl chain had (*S*)-directing effects and these effects were cumulative. However, there were several striking exceptions, especially for benzyl alkyl sulfides. [5c]

Scheme.

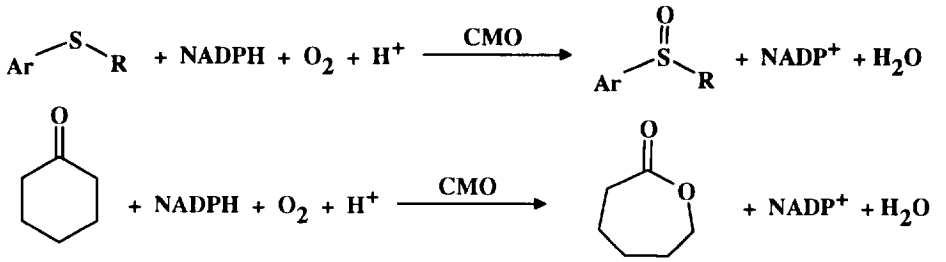

CMO, as can be inferred from its name, can also catalyze the oxidation of cyclohexanone to the corresponding lactone, by means of a Baeyer-Villiger reaction (**Scheme**). Several research groups have applied this reaction for resolution of racemic ketones and production of chiral lactones[6] and, in two cases,[6f,h] active site models for CMO have also been proposed. These two models were based on the hypothesis formulated by Walsh and Chen[7] that the oxygen transfer to the substrate takes place through a substrate-4a-hydroperoxy flavoenzyme complex.

In Furstoss' model,[6f,g] the active site was represented as a cube in which the substrate-hydroperoxyflavin complex was placed. The stereoselectivity was dictated by a "forbidden zone" localized inside the cube. In Taschner's model,[6h] predictions were based on the assumption that the substrate-hydroperoxyflavin complex was formed through a *Re* face attachment from the hydroperoxyflavin side, and an equatorial attachment from the ketone-ring side.

However, despite the significant advance that these models represent, the substrate range they cover is limited and cannot be applied to the case of sulfide oxidation, also with the hypothesis that the active site for Baeyer-Villiger oxidation is the same as that for sulfide oxidation. This prompted us to formulate an active site model that is predictive for the CMO catalyzed sulfide oxidation and that also includes the predictability of the other two models of Baeyer-Villiger activity.

Approach, description and application rules.

At present no structural data for CMO are available, but in order to further increase the application of the enzymatic oxidation method it is desirable to have a reliable model for predicting the specificity of this enzyme. To do this, the best strategy is to use the "cubic space" approach[8] for describing the active site based on substrate specificity studies, because this empirical approach does not require any structural information about the enzyme.

The **Table** shows the results we obtained in the CMO-catalyzed oxidation of about 30 sulfides, in terms of degrees of conversion into sulfoxides and enantiomeric excess and predominant absolute configuration of the products. It should be emphasized that the same results in terms of enantioselectivity were obtained with both crude and purified CMO, which demonstrates that the high sensitivity of CMO to

structural variations of the substrate is an intrinsic property of a single enzyme and that the crude preparation contains no other enzymes able to oxidize sulfides.[5c]

Table. CMO-catalyzed oxidation of sulfides to sulfoxides.

Entry	Sulfide	Conversion	e.e. (%)	Conf.	Reference
1	Ph-S-Me	88	99	R	5a
2	Ph-S-Et	86	47	R	5a
3	Ph-S-*n*Pr	54	68	S	5c
4	Ph-S-Vinyl	73	99	R	5b
5	Ph-S-*i*Pr	90	12	R	9
6	Bz-S-Me	97	54	R	5a
7	Bz-S-Et	80	67	S	5c
8	Bz-S-*n*Pr	90	96	S	5c
9	Bz-S-*n*Bu	98	15	S	5c
10	Bz-S-*i*Bu	90	90	S	5c
11	Bz-S-*i*Pentyl	95	80	S	5c
12	Bz-S-Hexyl	75	56	S	5c
13	*p*-(Me)-Bz-S-Me	97	5	R	5c
14	*p*-(Et)-Bz-S-Me	91	8	R	5c
15	*p*-(*i*Pr)-Bz-S-Me	88	4	R	5c
16	*p*-(*t*Bu)-Bz-S-Me	87	23	R	5c
17	*o*-(Me)-Ph-S-Me	90	87	R	5a
18	*m*-(Me)-Ph-S-Me	90	40	R	5a
19	*p*-(Me)-Ph-S-Me	94	37	S	5a
20	*p*-(Me)-Ph-S-Et	89	89	S	5a
21	*p*-(Me)-Ph-*i*Pr	99	86	S	5a
22	β-Naphthyl-S-Me	50	53	S	9
23	Ph-S-CH_2-CN	90	92	R	5b
24	Ph-S-CH_2-CH_2-CN	61	14	S	5b
25	*p*-(Me)-Ph-S-CH_2-CN	95	98	S	5b
26	*p*-(Me)-Ph-S-CH_2-CH_2-CN	71	61	S	5b
27	Ph-S- CH_2-CH_2Cl	75	93	S	5b
28	*p*-(Me)-Ph-S-CH_2-CH_2Cl	65	93	S	5b
29	*o*-Cl-Ph-S-Me	35	32	R	5a
30	*p*-Cl-Ph-S-Me	78	51	S	5a
31	*t*-Bu-S-Me	98	99	R	5a

The dimensions of the binding pockets were identified by superimposing the compound structures, as follows. Firstly, using the molecular modeling programme "HyperChem",[10] the total energy for the sulfoxide products was minimized (MM+[11]). We chose to work with the products for two main reasons: 1) to have an axis(S=O) from which to start to build up the model and 2) because it was possible to obtain extra information from the study of the configuration of the less abundant enantiomer. In order to superimpose the molecules, the products were divided into two families according to their predominant configuration. For each family, the molecules were aligned along the S=O bond and centered at the S atom and the two remaining fragments were then overlaid so as to occupy common volumes as far as possible, depending on the size of the groups. In a further step, these two clusters of molecules were put together, aligned again along the S=O bond and

centered at the S atom. At this point, however, the question arose about how to arrange the ends of this new cluster. The arrangement with four different ends, two for each configuration (*R* and *S*), was found to match the experimental evidence better than arrangements with two or three ends.

The three dimensional picture which emerged was then inserted inside a "cage" composed of several cubes of 1.54 Å edge.[8] In the model depicted in **Figure 1**, it is possible to see three binding loci and the catalytic site for the attack by the oxygen, which is delivered from the top. It can also be noted that two ends of the above mentioned cluster merged in the same locus, the main one. The molecules used to build this model are hydrophobic and thus polar effects are not taken into account. As a consequence, regions M (main), H_S (hydrophobic small) and H_L (hydrophobic large), are formally considered hydrophobic, and, therefore, forecasts for polar substrates would be poor. Also, the real boundaries for the three binding pockets have to be refined, and might well extend beyond the represented dimensions. The internal barriers that define the binding pockets are real physical constraints and cannot be penetrated by the substrate.

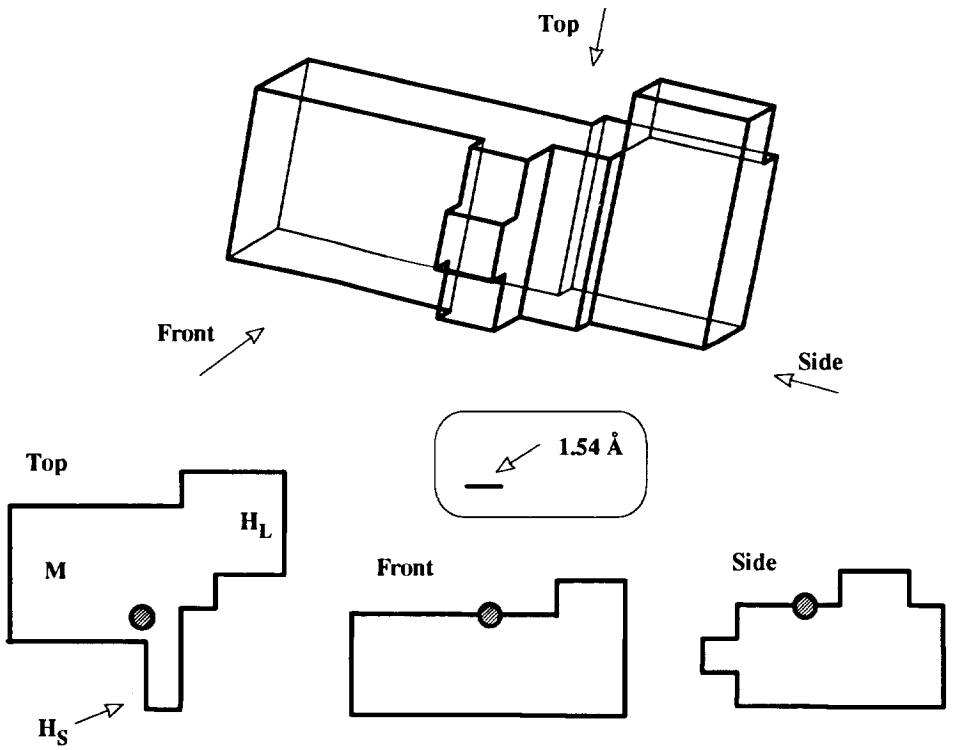

Figure 1. Active site model of CMO. The catalytically essential region (oxygen) is encircled. The top, front and side views are also shown, together with the scale. In the top view, the main (M), hydrophobic large (H_L) and hydrophobic small (H_S) pockets are depicted.

In the application of this model, and to keep it as simple as possible, the atoms are considered in point form and neither hydrogen atoms nor van der Waals radii are included. A few simple rules have to be followed in order to make predictions of the absolute configuration of the sulfoxide products:

1. The sulfur atom of the compound must be placed in the catalytic site aligned along the S=O axis, as if the reaction were taking place, with the oxygen occupying the circled region.

2. The two fragments of the molecule are then fitted into the most appropriate area of the model according to these guidelines:

a) the aromatic rings (or the largest fragments) will preferably occupy the M pocket for (*R*) configuration, unless they do not fit;

b) the smallest fragments will preferably occupy the H_S pocket for (*R*) configuration; if they do not fit in, they will go to the M pocket for an (*S*) configuration product;

c) the aromatic rings (or the largest fragments) that do not fit in the M pocket will fit in the H_L pocket (if possible).

It must be emphasized that this type of model cannot make predictions regarding the kinetic and quantitative features of the reactions such as V_{max}, K_m or yield.

Specific examples.

The application of the model to compounds **1-31** shows how the model can give us information about the stereoselectivities in CMO-catalyzed sulfide oxidations.

Phenyl alkyl sulfides. Alkyl chain influence.

Substrates **1-5** (**Table**) have the same aryl moiety but different alkyl ends. The preferred stereochemical reaction course is (*R*), with the exception of phenyl *n*-propyl sulfide (**3**), in which the first example of size-induced reversal of stereochemistry is observed.

Figure 2 depicts top projections of the above mentioned molecules. Part *a* shows phenyl methyl sulfide/sulfoxide in the active site, with the sulfur atom beneath the oxygen. It can be seen that when the aromatic ring, in accord with the application rules of the active site model, is placed in the M pocket, the methyl fragment fits the H_S pocket, which indicates (*R*) chirality. Analogous positioning can be adopted for entries **2**, **4** and **5**, which are all (*R*) derivatives (**Figure 2** *b*, *e*, *f*). Instead, with entry **3** the alkyl moiety does not fit in the H_S pocket (**Figure 2** *c*, and **Figure 1** in which the particular shape of H_S is shown better). This causes an alternative fitting inside the active site model, with the phenyl ring placed in the H_L pocket and the alkyl fragment in the M pocket giving the (*S*) configuration for the relative sulfoxide (**Figure 2** *d*). Also, the low value of the (*R*) enantiomeric excess for entry **5** tells us that the H_S pocket is tailored for small size fragments. In this case there is an almost complete lack of discrimination (12% e.e.) because the *iso*-propyl fragment bumps against the H_S walls.

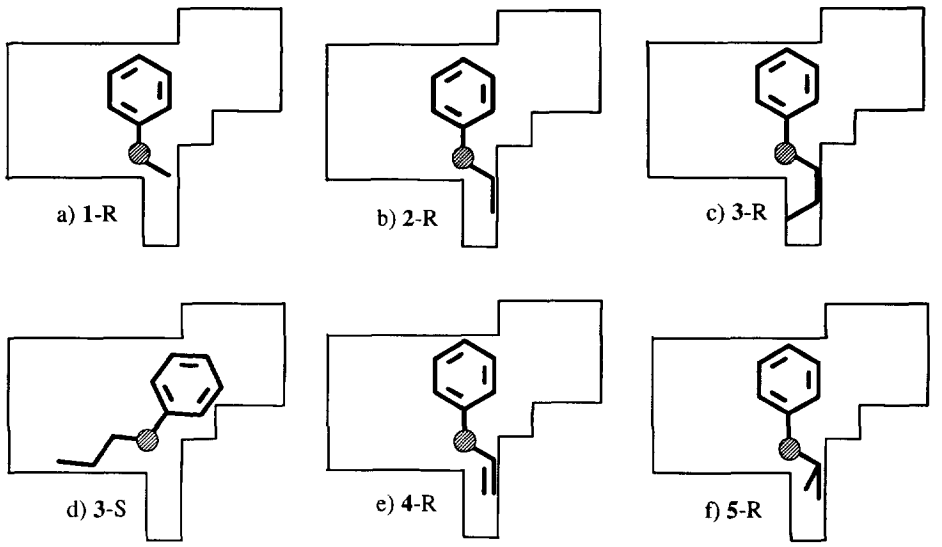

Figure 2. Top perspective view of the active site model showing the preferred binding modes for phenyl alkyl sulfides **1-5**.

Benzyl alkyl sulfides. Alkyl chain influence.

From the active site model and from what we have already learned about the size of the H_S pocket, it is not difficult to place benzyl derivatives **6-12** (**Table**) in the model (**Figure 3**). The hydrophobic interactions of the aromatic ring in the M pocket are weaker for phenyl than for benzyl derivatives and this increases the influence of the alkyl fragment in inducing stereospecificity.

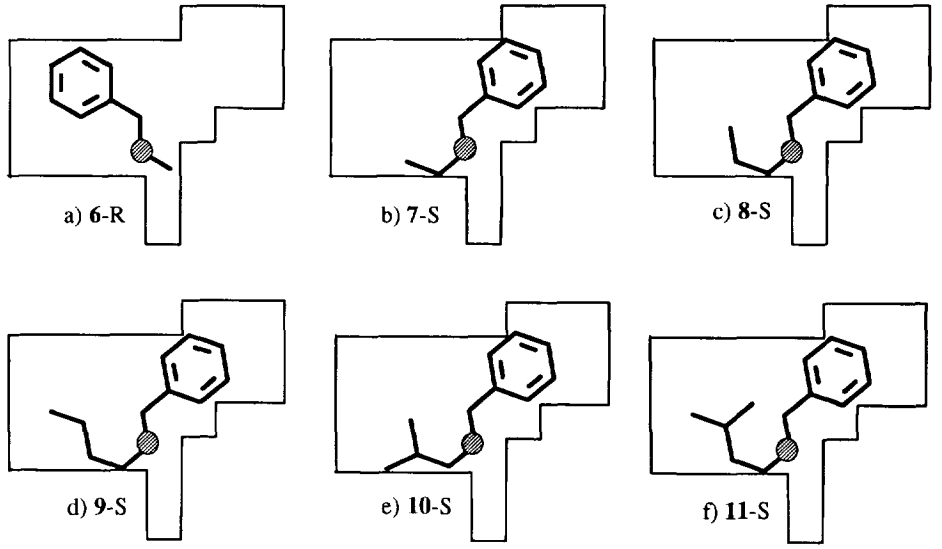

Figure 3. Top perspective view of the preferred binding modes for benzyl alkyl sulfides **6-11**.

Therefore, the presence of an ethyl group is enough to invert the stereochemical course from (*R*) to (*S*). However, the discrepancies of the correlation between enantiomeric excess values and alkyl chain size (**Table**) suggest that some factor other than bulkiness also influences the stereochemistry.

p-Alkylbenzyl methyl sulfides. p-Alkyl chain influence.

The *para* substituted benzyl methyl of entries **13-16** (**Table**) give nearly racemic sulfoxides with only a slight (*R*) preference. This suggests that, in the (*R*) configuration, the chain in *para* position does not fit comfortably in the M pocket, making the fitting of the opposite configuration in the H_L pocket almost equally favored (**Figure 4**). These data give information useful for setting the boundaries of the M pocket and also give the minimal size for the H_S pocket.

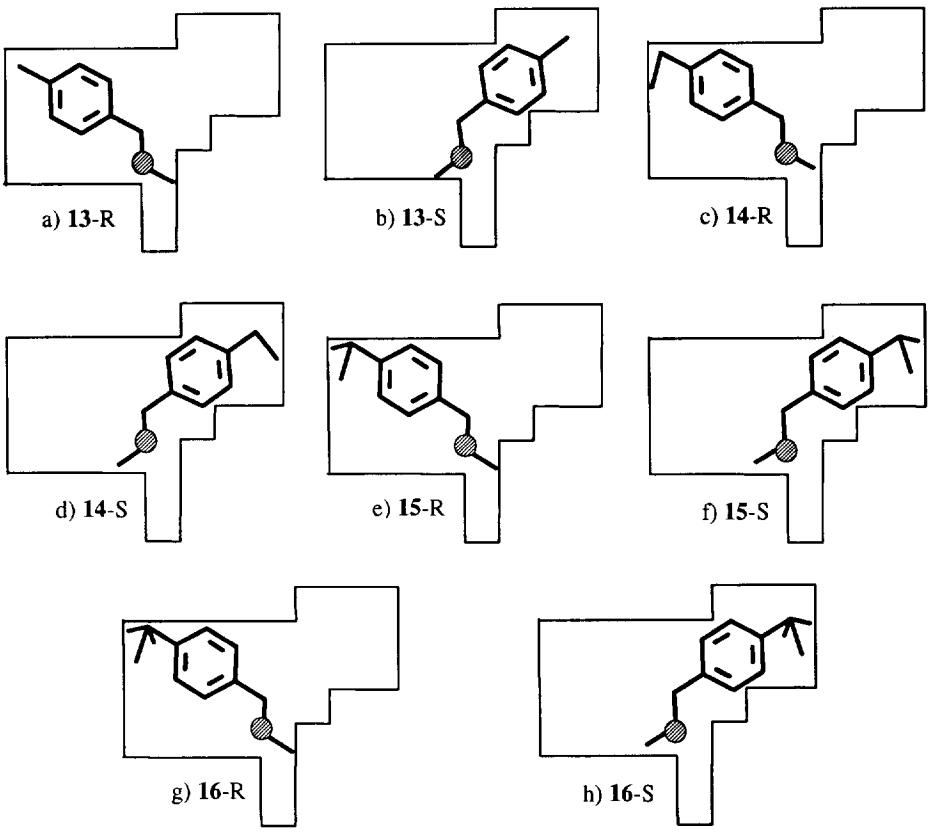

Figure 4. Top perspective view of the preferred binding modes of *p*-alkylbenzyl methyl sulfides **13-16**.

Alkylphenyl alkyl sulfides.

These compounds (**17-22**, **Table**) are substituted in different positions of the aromatic ring. In **Figure 5** *a*, the (*R*) configuration of the *o*-, *m*- and *p*-methyl phenyl-derivatives is represented in the active site model.

It must be noted that the *para*-substituent protrudes outside the M pocket, making the (*R*) structure unable to fit the model. The fit is better for the (*S*) structure (**Figure 5** *b*). Analogously, for **20-21** the only permitted configuration is the (*S*) one, and the presence of a bulkier alkyl moiety increases the e.e. values. With the β-naphthyl derivative, which can be considered a special *m,p*- substituted phenyl derivative, the preferred fit inside the active model is again the one with (*S*) chirality.

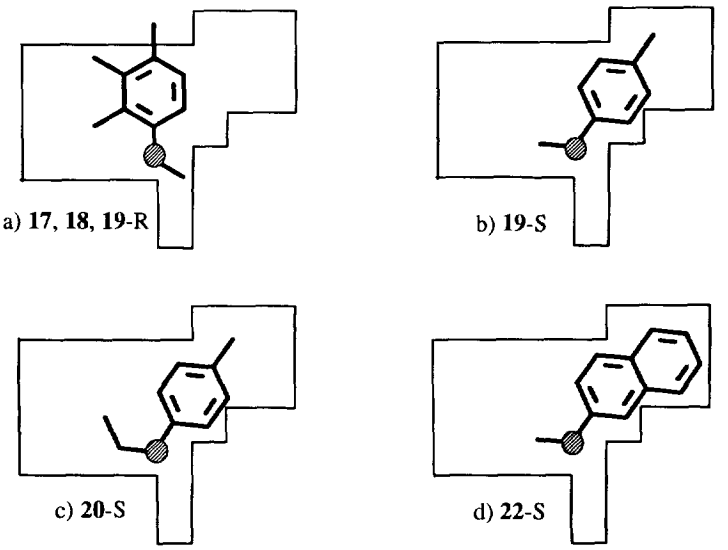

Figure 5. Top perspective view of the preferred binding modes of alkylphenyl alkyl sulfides **17-22**.

Cyano and chloro substituted phenyl alkyl sulfides.

These derivatives (**23-30**), which have cyano and chloro substituents in various positions, show chiralities in accord with the size-induced stereochemistry of the model. It is reasonable to obtain (*R*) derivatives for **23** and **29**, since the alkyl chain is relatively small and the *para* position is free. The other substrates (**24**, **27** and **28**) fit well in the (*S*) configuration at sulfur atom, induced by chain bulkiness and (or) *para* substituents. It can not be ruled out that e.e. values are also influenced somewhat by electronic factors, which are not taken into account in this model.

Dialkyl sulfides.

t-Butyl methyl sulfide (**31**) is a good substrate for CMO, which yields the sulfoxide with the (*R*) configuration. This compound is very important for the determination of the vertical thickness of the model, as can be seen from the front view of the compound inside the model (**Figure 6** *b*).

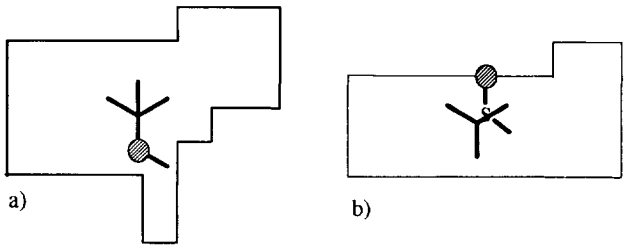

Figure 6. Top (*a*) and front (*b*) perspective views of the preferred binding mode of *t*-butyl methyl sulfide **31**.

Comparison with other models.

For the CMO-catalyzed Baeyer-Villiger reaction, two excellent initial formulations of active site models have been published so far.[6f,h] This reaction consists of a ketone oxidation followed by a C-C migration which leads to an optically enriched lactone. Since the same flavin is responsible for the oxidation of ketone and sulfur, it turns out that the active site for these two distinct reactions is the same, even though the interacting areas can be different for the two cases.

Furstoss' model[6f,g] is mainly based on Deslongchamps statement[12] that in a chemical Baeyer-Villiger oxidation the migration of the C-C bond is antiperiplanar to the leaving group. Furstoss localizes a "forbidden zone" in the active site model that limits the number of the possible configurations of cyclic ketones and therefore leads to a preferred C-C migration. **Figure 7** represents the case of two enantiomeric bicyclic ketones inside our model: *a* and *b*, depict two possible dispositions of one of the two enantiomers at the catalytic site. It is evident that case *b* does not fit in our model, because the compound falls outside the model, in an area which can be considered equivalent to the "forbidden zone" of Furstoss. For the other enantiomer two dispositions are again possible (*c* and *d*). From the literature[6g] it is known that the compound deriving from disposition *c* is the major one. This is in agreement with our model, since case *c* is similar to case *a*, with the hydroxy group (formed from the ketone group upon attack by the hydroperoxyflavin) directed toward H_S and the rest of the molecule rotated 90° inside the M pocket. Instead, in *d*, the hydroxy group is directed toward the M pocket and the rest of the molecule partially bumps against one of the walls of the model which is unfavorable to this accommodation. These results tell us that the H_S pocket is probably the natural pocket for the hydroxy group (see case *a* and *c*) and therefore a site containing polar elements. As shown for sulfides, it can also accommodate the methyl group or small hydrophobic groups, but increase of the hydrophobic component decreases the e.e. values of the (*R*) enantiomer (**Table**).

The model proposed by Taschner et al.[6h] was prompted by the striking sequence homology between the flavin-binding domain of CMO and those of human and *E.Coli* glutathione reductases, whose X-ray crystal structures are available.[7,13] By analogy, the same *re* facial attachment of hydroperoxide to the flavin was also assumed for CMO. This, together with Deslongchamps rule,[12] was the basis of the active model. Taschner suggested that between axial and equatorial attachment, the equatorial attachment of 4a-hydroperoxide-flavin

to the ketone ring is favored, because of a possible hydrogen bond between the hydroxy group of the substrate transition state and the carbonyl group of the flavin.

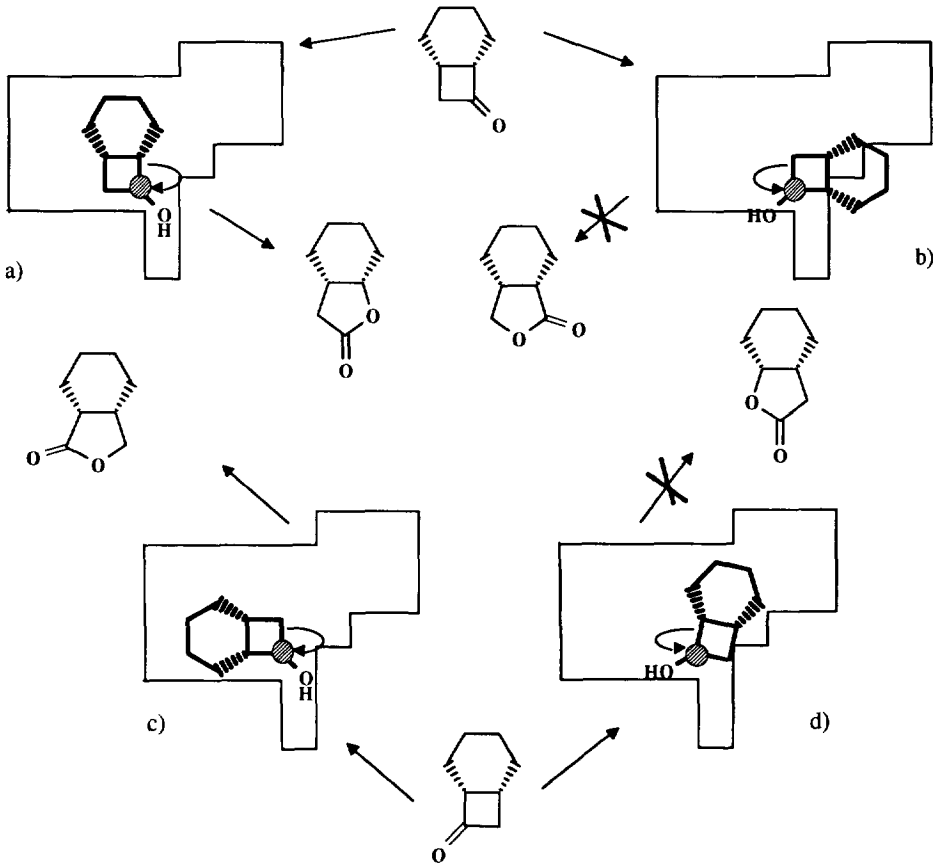

Figure 7. Top perspective view of the preferred binding modes in CMO catalyzed Baeyer-Villiger oxidation of racemic bicyclic ketones.

Figure 8 depicts how this situation works in our model. Again, the hydroxy group points toward H_S forming a hydrogen bond with the carbonyl group of the flavin, and this also determines the flavin position. The hydrogen bond is clearly depicted in the side view of the model (**Figure 8** *b*).

The present model is perfectly compatible with the substrate-flavin arrangements proposed by Taschner, with the flavin moiety localized outside the cage.

Very recently, another active site model for Baeyer-Villiger reactions, based on the stereochemistry of the hydroxyperoxide intermediate, has been proposed.[14]

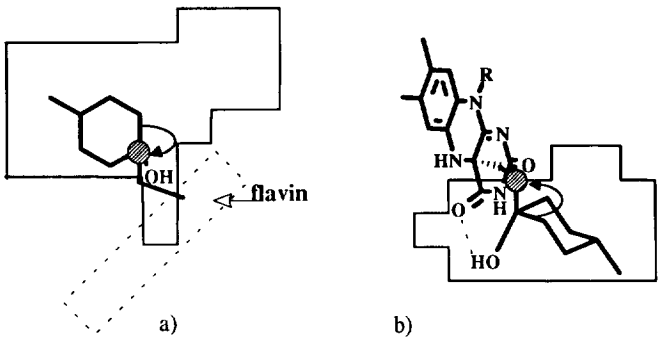

Figure 8. Top (a) and side (b) perspective views of the preferred binding modes of the 4a-hydroperoxyflavin-4-methylhexanone complex.

Conclusions.

The proposed active site model for CMO was established with a wide range of sulfide/sulfoxide structures and can be used, when following the rules for application, to predict with fairly good confidence the stereochemical course of CMO-catalyzed oxidation of hydrophobic compounds. Work is in progress to further delineate the size of the pockets and to accommodate the introduction of polar effects.

In addition, this model is also suitable for interpreting CMO catalyzed Baeyer-Villiger oxidations, and assuming that the H_S pocket preferentially accommodates the hydroxy group, it appears consistent with the other previously described models.[6f,h] More substrates, however, should be checked before assuming that the present model is really reliable for Baeyer-Villiger reactions.

It should also be emphasized that the model can be easily built with any molecular kit, facilitating the rapid interpretation and stereochemical prediction of CMO-catalyzed reactions.

Acnowledgements.

We are grateful to Professor J.B. Jones (University of Toronto) for helpful suggestions and criticism.

References and Notes.

1 a) Auret, B.J.; Boyd, D.R.; Henbest, H.B.; Ross, S.; *J. Chem. Soc.*, **1968**, 2371. b) Abushanab, E.; Reed, D.; Suzuki, F.; Sih, C.J.; *Tetrahedron Lett.*, **1978**, 3415. c) Holland, H.L.; Popperl, H.; Ninniss, R.W.; Chenchaiah, P.C.; *Can. J. Chem.*, **1985**, *63*, 1118. d) Ohta, H.; Okamoto, Y.; Tsuchihashi, G.I.; *Agric. Biol. Chem.*, **1985**, *49*, 671. e) Rossi, C.; Fauve, A.; Madesclaire, M.; Roche, D.; Davies, F.A.; Reddy, R.T.; *Tetrahedron Asymmetry*, **1992**, *3*, 629. f) Colonna, S.; Gaggero, N.; Manfredi, A.; Casella, L.; Gullotti, M.; Carrea, G.; Pasta, P.; *Biochemistry*, **1990**, *29*, 10465. g) Colonna, S.; Gaggero, N.; Casella, L.; Carrea, G.; Pasta, P.; *Tetrahedron Asymmetry*, **1992**, *3*, 95. h) Colonna, S.; Gaggero, N.; Carrea, G.; Pasta, P.; *J. Chem. Soc. Chem. Commun.*, **1992**, 357. i) Light, D.R.; Waxman, D.J.; Walsh, C.; *Biochemistry*, **1982**, *21*, 2490. l) Walsh, C.T.; Chen, Y.-C.J.; *Angew. Chem. Int. Ed. Engl.*, **1988**, *27*, 333. m)Holland, H.L.; *Chem. Revs.*, **1988**, *88*, 473.

2 a) Zhao, S.H.; Samuel, O.; Kagan, H.B.; *Tetrahedron*, **1987**, *43*, 5135. b) Di Furia, F.; Modena, G; *Synthesis*, **1984**, 325. c) Rebiere, F.; Samuel, O.; Ricard, L.; Kagan, H.B.; *J. Org. Chem.*, **1991**, *56*, 5991.

3 Marino, J.P.; Bogdan, S.; Kimura, K.; *J. Am. Chem. Soc.*, **1992**, *114*, 5566.

4 a) Solladié, G.; *Synthesis*, **1981**, 185. b) Drabowicz, J.; Kielbasinski, P.; Mikolajczyk, M.; in: *The Chemistry of Sulphones and Sulphoxides*. Patai, S., Rappoport, Z. and Stirling, C.J.M. Eds., John Wiley & Sons Ltd., **1988**, p233. c) Cinquini, M.; Cozzi, F.; Montanari, F.; in: *Organic Sulfur Chemistry*. Bernardi, F., Csizmadia, I.G. and Mangini, A. Eds., Elsevier, **1985**, p. 355.

5 a) Carrea, G.; Redigolo, B.; Riva, S.; Colonna, S.; Gaggero, N.; Battistel, E.; Bianchi, D.; *Tetrahedron Asymmetry*, **1992**, *3*, 1063. b) Secundo, F.; Carrea, G.; Dallavalle, S.; Franzosi, G.; *Tetrahedron Asymmetry*, **1993**, *4*, 1981. c) Pasta, P.; Carrea, G.; Holland, H.L.; Dallavalle, S.; *Tetrahedron Asymmetry*, **1995**, *6*, 993.

6 a) Ouazzani-Chahdi, J.; Buisson, D.; Azerad, R.; *Tetrahedron Lett.*, **1987**, *28*, 1109. b) Taschner, M.J.; Black, D.J.; *J. Am. Chem. Soc.*, **1988**, *110*, 6892. c) Abril, O.; Ryerson, C.C.; Walsh, C.; Whitesides, G.M.; *Bioorg. Chem.*, **1989**, *17*, 41. d) Levitt, M.; Sandey, H.; Willets, A.; *Biotechnol. Lett.*, **1990**, *12*, 197. e) Königsberger, V.; Alphand, V.; Furstoss, R.; Griengl, H.; *Tetrahedron Lett.*, **1991**, *32*, 449. f) Furstoss, R.; in: *Microbial Reagents in Organic Synthesis*. S. Servi Ed. Kluwer Academic Publisher, **1992**, p333. g) Alphand, V.; Furstoss, R.; *J. Org. Chem.*, **1992**, *57*, 1306. h) Taschner, M.J.; Peddada, L.; Cyr, P.; Chen, Q.-Z.; Black, D.J.; in: *Microbial Reagents in Organic Synthesis*. S. Servi Ed. Kluwer Academic Publisher, **1992**, p347. i) Gagnon, R.; Grogan, G.; Levitt, M.S.; Roberts, S.M.; Wan, P.W.H.; Willets, A.J.; *J. Chem. Soc. Perkin Trans. I*, **1994**, 2537.

7 Walsh, C.T.; Chen, Y.-C.J.; *Angew. Chem. Int. Ed. Engl.*, **1988**, 27, 333.

8 a) Jones, J.B.; Jakovac, I.J.; *Can. J. Chem.*, **1982**, *60*, 19. b) Toone, E.J.; Werth, M.J.; Jones, J.B.; *J. Am. Chem. Soc.*, **1990**, *112*, 4946. c) Provencher, L.; Wynn, H.; Jones, J.B.; Krawczyk, A.R.; *Tetrahedron Asymmetry*, **1993**, *4*, 2025. d) Provencher, L.; Jones, J.B.; *J. Org. Chem.*, **1994**, *59*, 2729.

9 Sulfides **5** and **22** were synthesized as previously reported (Holland, H.L.; Brown, F.M.; Larsen, B.G.; *Bioorg. Medicinal Chem.*, **1994**, *4*, 647. Staudinger, H.; Goldstein, H.; Schlenker, E.; *Helv.Chim.Acta*, **1921**, *4*, 342). The enzymatic oxidation was carried out as follows: the sulfide (0.1 mmol) was magnetically stirred in 4 ml of 0.05 M Tris-HCl buffer, pH 8.6, containing 2 μmol NADPH, 0.4 mmol glucose-6-phosphate, 5 units of CMO and 10 units of glucose-6-phosphate dehydrogenase. After overnight reaction, the solution was extracted with 4 portions (4 ml each) of ethyl acetate and the organic extract was dried and evaporated. The enantiomeric excess of sulfoxides were determined by chiral HPLC on a Chiracel OB (sulfoxide obtained from **5**) or OD (sulfoxide obtained from **22**) column, using the proper mixture of *n*-hexane and propan-2-ol as the mobile phase. The absolute configuration was determined by comparison with authentic samples (Holland, H.L.; Brown, F.M.; Larsen, B.G.; *Bioorg. Medicinal Chem.*, **1994**, *4*, 647. Palucki, M.; Haunson, P.; Jacobsen, E.N.; *Tetrahedron Lett.*, **1992**, *33*, 7111) using chiral HPLC.

10 HyperChem from HYPERCUBE INC. Waterloo, Ontario, Canada.

11 Allinger, N.L.; *J. Am. Chem. Soc.*, **1977**, *99*, 8127.

12 Deslongchamps, P.; in: *Stereoelectronic effects in Organic Chemistry*. Permagon Press, **1983**.

13 Wieranga, R.K.; Drenth, J.; Schulz, G.E.; *J. Mol. Biol.*, **1983**, *167*, 725.

14 Kelly, D.R.; Knowles, C.J.; Mahdi, J.G.; Taylor, I.N.; Wright, M.A.; *J. Chem. Soc., Chem. Commun.*, **1995**, 729.

(*Received in UK* 20 *April* 1995)